

Charge-transfer cross sections in collisions of Be^{q+} ($q=1-4$) and B^{q+} ($q=1-5$) with ground-state atomic hydrogen

M. Das

Department of Theoretical Physics, IACS, Calcutta 700032, India

M. Purkait and C. R. Mandal

Department of Physics, Jadavpur University, Calcutta 700032, India

(Received 11 December 1997)

A prior form of boundary corrected continuum intermediate state approximation has been employed to calculate charge-transfer cross sections involving different degree ions of beryllium and boron with atomic hydrogen in the energy range of 25–200 keV/amu. In this formalism, interactions of the active electron with the partially stripped ions have been estimated by a model potential. Results agree favorably well with the available results in some processes. In other processes results have been reported. [S1050-2947(98)04305-4]

PACS number(s): 34.70.+e

I. INTRODUCTION

Studies on inelastic collision processes involving multi-charged ions and atomic hydrogen have attracted a great deal of experimental and theoretical works [1–7] due to their diverse applications on different branches of physics, viz., astrophysics, fusion research etc. during the last two decades. Very recently beryllium and boron have been identified as the plasma facing materials replacing high-Z surface materials such as Ni, Fe, and Mo in the next step fusion reactors such as ITER. For this reason, a very accurate atomic database of cross sections of different inelastic processes involving ions of beryllium and boron with atomic hydrogen is required over the entire range of collisional energies. Accurate cross sections for the inelastic processes involving fully stripped ions of beryllium and boron with atomic hydrogen are available in the literature. In contrast, not much cross-section data are available for the inelastic processes involving partially stripped ions of beryllium and boron with atomic hydrogen where the interactions of such partially stripped ions with atomic hydrogen are very complicated in nature. Of the inelastic processes, we shall focus our attention only on the charge-transfer phenomenon involving different degree ions of beryllium and boron with ground-state atomic hydrogen.

Olson and Salop [8] have calculated the charge-transfer cross sections in collisions of B^{q+} , C^{q+} , N^{q+} , and O^{q+} ($q \geq 3$) with atomic hydrogen in the framework of classical trajectory Monte Carlo simulation (CTMC) method in the intermediate- and high-energy regions. Subshell results are not available from their investigations. Hansen and Dubois [9] have employed a two center atomic-state expansion method to study charge-transfer cross sections in $\text{B}^{q+} + \text{H}$ or He ($q=1,3,5$) interactions in the energy range of 0.1 to 100 keV/amu. Cross sections for charge transfer into different subshells of the projectile ions are available from their calculations. However, they are confined to closed-shell or sub-shell ions of boron only. Schultz *et al.* [10] have calculated all the inelastic cross sections in collisions of Be^{q+} ($q=2-4$) with atomic and molecular hydrogen in the energy

range of 1 keV/amu–1 MeV/amu in the framework of the CTMC method and charge-transfer cross sections to each individual subshell have been given in tabular form. Under the prevailing circumstances we are motivated to study charge-transfer cross sections for the interaction of Be^{q+} (B^{q+}) with atomic hydrogen in the intermediate- and high-energy regions. We have formulated our problem in the framework of the boundary corrected continuum intermediate state (BCCIS) approximation originally proposed by Mandal *et al.* [11]. The essence of this method lies in the following facts: (i) Intermediate continuum states have been incorporated into the formalism, (ii) boundary conditions are satisfied correctly, and (iii) formulation may be extended easily to non-Coulombic interactions as well.

The organization of the paper is as follows. In Sec. II, theoretical formulation, evaluation of the matrix element, and construction of the model potential are given. Results and discussions are the contents of Sec. III. Finally concluding remarks are given in Sec. IV.

Atomic units are used throughout unless otherwise stated.

II. THEORY

A collisional diagram is shown in Fig. 1. The total Hamiltonian for the whole system may be written as

$$H = H_0 + V_{Te}(\vec{r}_T) + V_{Pe}(\vec{r}_P) + V_{TP}(\vec{R}), \quad (1)$$

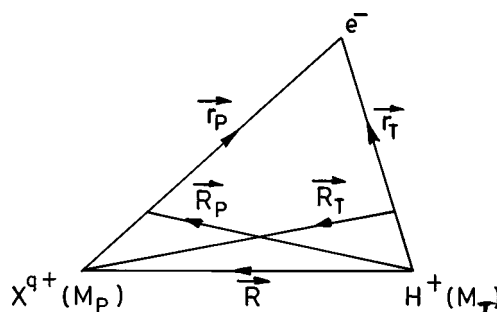


FIG. 1. Coordinate representation for the reaction $X^{q+} (\text{Be}^{(1-4)+}$ or $\text{B}^{(1-5)+}) + \text{H}(1s) \rightarrow X^{(q-1)+}(nl) + \text{H}^+$.

where H_0 is the kinetic energy term, which has as usual different forms in the entrance and exit channels, respectively and V represents the pair interaction labeled by subscripts in a charge-transfer reaction where e , T , and P represent active electron, target ion, and projectile ion, respectively.

The prior form of the transition amplitude in the framework of the BCCIS approximation may be written as

$$T_{if}^{(-)} = \langle \psi_f^{\text{BCCIS}} | V_{TP}(\vec{R}) + V_{Pe}(\vec{r}_P) | \psi_i \rangle, \quad (2)$$

$$\psi_f^{\text{BCCIS}}(\text{Prior}) = N e^{i\vec{k}_f \cdot \vec{R}_P} \phi_f(\vec{r}_P) {}_1F_1(-i\nu_1; 1; -ia(v_f r_i + \vec{v}_f \cdot \vec{r}_T)) {}_1F_1(i\nu_2; 1 - ib(k_f R_T + \vec{k}_f \cdot \vec{R}_T)), \quad (4)$$

where

$$N = (b\mu_f)^{i\nu_1} e^{(\pi/2)(\nu_1 - \nu_2)} \Gamma(1 + i\nu_1) \Gamma(1 - i\nu_2),$$

$$a = \frac{M_T}{1 + M_T}, \quad b = \frac{M_P}{1 + M_P}, \quad \mu_f = \frac{M_T(M_P + 1)}{M_T + M_P + 1},$$

$$\nu_1 = \frac{1}{v_f}, \quad \nu_2 = \frac{q}{v_f}.$$

In the case of heavy particle collision, it has been shown [12] that

$${}_1F_1(i\nu_2; 1; -ib(k_f R_T + \vec{k}_f \cdot \vec{R}_T)) \approx {}_1F_1(i\nu_2; 1; -ib(k_f R_P + \vec{k}_f \cdot \vec{R}_P)).$$

Now it is trival to show that the asymptotic form of the total wave function may be written as

$$\lim_{R_P \rightarrow \infty} \psi_f^{\text{BCCIS}}(\text{prior}) = N \phi_f(\vec{r}_P) e^{i\vec{k}_f \cdot \vec{R}_P - [i(q-1)/v_f] \ln(k_f R_P + \vec{k}_f \cdot \vec{R}_P)}. \quad (5)$$

A. Construction of the interacting two-body potentials and final bound-state wave function

There is no ambiguity in the construction of $V_{Te}(\vec{r}_T)$ and it is uniquely determined by the Coulomb potential. The interaction of the active electron and the projectile ion of charge q has been described in three different ways as follows.

The projectile ion has been treated as a rigid core ion due to screening by the passive electrons and the charge (Z_P) on the projectile ion is determined by (i) binding energy screening [13,14] (BES), i.e., $Z_P = (-2n_f^2 \epsilon_f)^{1/2}$, where ϵ_f is the binding energy of the electron in the final state represented by principal quantum number n_f , and (ii) slater screening [13,14] (SS), i.e., $Z_P = Z - \sigma$, where Z is the nuclear charge of the projectile and σ [15] is the total screening charge by the passive electrons. In these two cases, the final-state wave function is hydrogenic with nuclear charge Z_P . (iii) In other

cases, the interaction of the active electron with the projectile ion has been estimated by a model potential as

$$\psi_i = e^{i\vec{k}_i \cdot \vec{R}_T} \phi_i(\vec{r}_T) \quad (3)$$

where ψ_i is the unperturbed wave function in the entrance channel and may be written as

$$\psi_f^{\text{BCCIS}}$$

is the approximate form (prior) of the total wave function of the whole collisional system in the on-shell approximation and may be written as

$$V_{Pe}(\vec{r}_P) = -\frac{q}{r_P} - \frac{e^{-\lambda r_P}}{r_P} \{(Z - q) + br_P\}, \quad (6)$$

where Z and q are respectively the nuclear and asymptotic charge of the projectile ion. b and λ are two arbitrary parameters chosen variationally with respect to a slater basis set in such a way that the corresponding Hamiltonian of the active electron in the final state is diagonalized to reproduce correct binding energies. These binding energies of the active electron on different projectile ions are calculated from the tables of Clementi and Roetti [16] and works of Clark and Abdallah [17]. Potential parameters for different projectile ions are given in Table I. It has been observed that a unique set of parameters for the potential reproduce binding energies of the captured electron in a different subshell with better accuracy for a particular shell of the projectile ion, which has initially a closed shell or subshell structure. For the capture to the open shell of the projectile ion, potential parameters have to change a little to find out the binding energies of the active electron in each different subshell to which the capture occurs. However, to check the accuracy of the wave function, the virial theorem has been tested and is found to be accurate within 0.01% in all cases.

With the assumption of the rigid core of the projectile ion [cases (i) and (ii)], it is obvious that the interaction of the projectile ion with the target nucleus should be Coulombic. In case (iii) also, we have treated the interaction of the

TABLE I. Model potential parameters λ and b in Eq. (6) are given for different ions.

Ion	λ	b
Be ⁺	2.3292	3.8616
Be ²⁺	4.3792	3.4616
Be ³⁺	6.5792	2.3446
B ⁺	2.1435	4.4119
B ²⁺	3.4012	5.8235
B ³⁺	6.2512	5.8616
B ⁴⁺	7.0512	8.2616

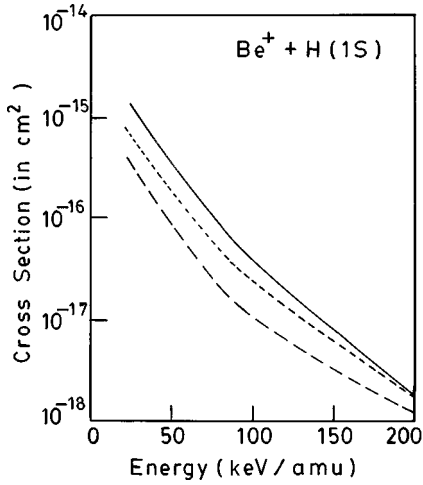


FIG. 2. Total capture cross sections for $\text{Be}^+ + \text{H}(1s)$ collisions. Theory: —, present work with model potential; · · · ·, present work with SS model; - - -, present work with BES model.

jectile ion and the target nucleus as a Coulomb interaction between two charges of magnitude q and 1, respectively. This is well justified even if some short-range part exists that will not affect the charge-transfer cross sections.

B. Evaluation of the transition amplitude

The transition amplitude in the framework of the BCCIS approximation may be written as

$$T_{if}^{(-)} = N \int d\vec{r}_T d\vec{R}_T e^{-i\vec{k}_f \cdot \vec{R}_P} \phi_f^*(\vec{r}_P) {}_1F_1(iv_1; 1; ia(v_f r_T + \vec{v}_f \cdot \vec{r}_T)) {}_1F_1(-iv_2; 1; ib(k_f R_T + \vec{k}_f \cdot \vec{R}_T)) \times [V_{TP}(\vec{R}) + V_{Pe}(\vec{r}_P)] e^{i\vec{k}_i \cdot \vec{R}_T} \phi_i(\vec{r}_T). \quad (7)$$

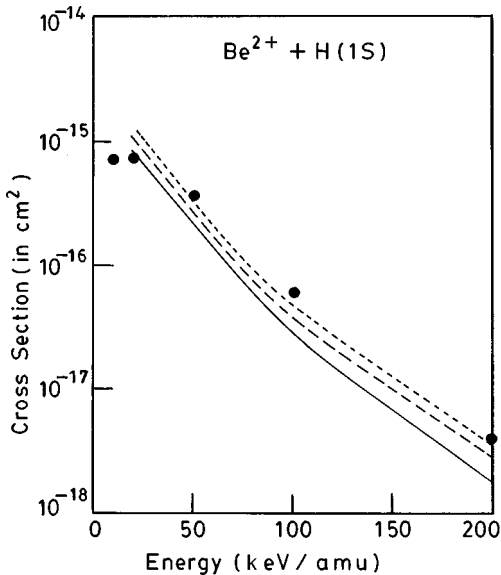


FIG. 3. Total capture cross sections for $\text{Be}^{2+} + \text{H}(1s)$ collisions. Theory: —, present work (model potential); · · · ·, present work (SS model); - - -, present work (BES model); and ●'s, CTMC results of Schultz *et al.* [10].

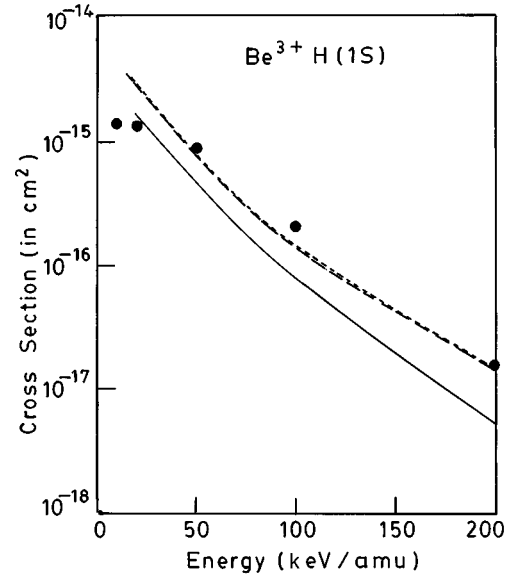


FIG. 4. Total capture cross sections for $\text{Be}^{3+} + \text{H}(1s)$ collisions. Theory: —, present work (model potential); · · · ·, present work (SS model); - - -, present work (BES model); and ●'s, CTMC results of Schultz *et al.* [10].

As per the discussions in Sec. II A, the form of $V_{TP}(\vec{R}) + V_{Pe}(\vec{r}_P)$ may be written as follows: For cases (i) and (ii),

$$V_{TP}(\vec{R}) + V_{Pe}(\vec{r}_P) = \frac{Z_P}{R} - \frac{Z_P}{r_P}. \quad (8)$$

For case (iii),

$$V_{TP}(\vec{R}) + V_{Pe}(\vec{r}_P) = \frac{q}{R} - \frac{q}{r_P} - \frac{e^{-\lambda r_P}}{r_P} (a + b r_P), \quad (9)$$

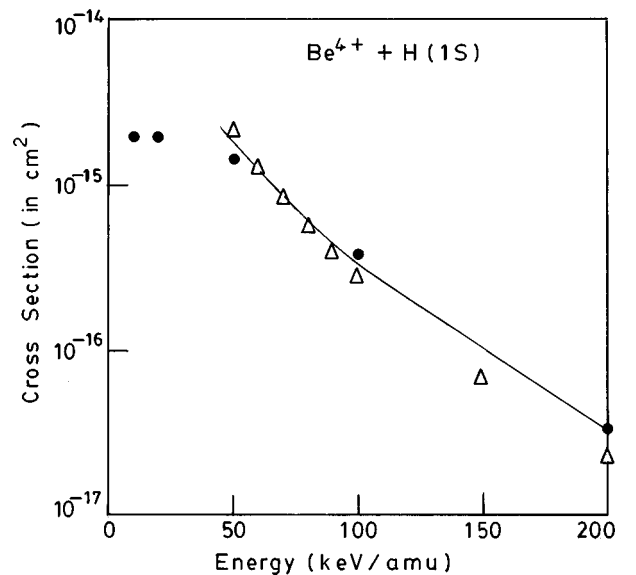


FIG. 5. Total capture cross sections for $\text{Be}^{4+} + \text{H}(1s)$ collisions. Theory: —, present work; $\Delta\Delta\Delta$, the results of CDW-EFS method of Busnengo *et al.* [19]; and ●●●●, CTMC results of Schultz *et al.* [10].

TABLE II. Total nl cross sections for $\text{Be}^+-\text{H}(1s)$ ($a[b]$ stands for $a \times 10^b$).

Energy (keV/amu)	Cross sections (10^{-16} cm^2)							Total
	$2s$	$2p$	$Q(2)$	$3s$	$3p$	$3d$	$Q(3)$	
25	3.36[0]	8.06[0]	1.14[+1]	8.37[-2]	6.36[-2]	7.05[-3]	1.54[-1]	1.16[+1]
30	2.64[0]	6.89[0]	9.53[0]	8.44[-2]	5.75[-2]	6.16[-3]	1.48[-1]	9.68[+0]
40	1.57[0]	4.38[0]	5.95[0]	6.70[-2]	4.09[-2]	3.93[-3]	1.12[-1]	6.06[+0]
50	9.44[-1]	3.70[0]	4.64[0]	4.64[-2]	2.64[-2]	2.30[-3]	7.51[-2]	4.72[+0]
60	5.75[-1]	1.59[0]	2.16[0]	3.12[-2]	1.66[-2]	1.33[-3]	4.91[-2]	2.21[+0]
80	2.35[-1]	6.15[-1]	8.50[-1]	1.39[-2]	6.49[-3]	4.50[-4]	2.08[-2]	8.71[-1]
100	1.06[-1]	2.59[-1]	3.65[-1]	6.62[-3]	2.77[-3]	1.72[-4]	9.56[-3]	3.74[-1]
200	5.47[-3]	1.12[-2]	1.67[-2]	3.97[-4]	1.04[-4]	4.19[-6]	5.05[-4]	1.72[-2]

TABLE III. Total nl cross sections for $\text{Be}^{2+}-\text{H}(1s)$ ($a[b]$ stands for $a \times 10^b$).

Energy (keV/amu)	Cross sections (10^{-16} cm^2)							Total
	$2s$	$2p$	$Q(2)$	$3s$	$3p$	$3d$	$Q(3)$	
25	1.78[0]	3.28[0]	5.06[0]	2.26[-1]	9.12[-1]	4.63[-1]	1.60[0]	6.66[0]
30	1.33[0]	2.48[0]	3.81[0]	2.01[-1]	8.67[-1]	4.16[-1]	1.48[0]	5.29[0]
40	7.72[-1]	1.48[0]	2.20[0]	1.48[-1]	6.57[-1]	2.78[-1]	1.08[0]	3.28[0]
50	4.68[-1]	8.58[-1]	1.33[0]	1.06[-1]	4.54[-1]	1.71[-1]	7.31[-1]	2.06[0]
60	2.94[-1]	5.32[-1]	8.26[-1]	7.68[-2]	3.06[-1]	1.03[-1]	4.56[-1]	1.30[0]
80	1.28[-1]	2.26[-1]	3.54[-1]	4.17[-2]	1.40[-1]	3.95[-2]	2.21[-1]	5.75[-1]
100	6.15[-2]	1.07[-1]	1.68[-1]	2.38[-2]	6.74[-2]	1.64[-2]	1.08[-1]	2.76[-1]
200	3.87[-3]	6.97[-3]	1.08[-2]	2.56[-3]	3.80[-3]	5.72[-4]	6.93[-3]	1.77[-2]

TABLE IV. Total nl cross sections $\text{Be}^{3+}-\text{H}(1s)$ ($a[b]$ stands for $a \times 10^b$).

Energy (keV/amu)	Cross sections (10^{-16} cm^2)								
	$1s$	$Q(1)$	$2s$	$2p$	$Q(2)$	$3s$	$3p$	$3d$	$Q(3)$
25	6.39[-3]	6.39[-3]	2.05[0]	2.49[0]	4.54[0]	4.97[-1]	2.06[0]	3.58[0]	6.14[0]
30	5.03[-3]	5.03[-3]	1.47[0]	1.82[0]	3.29[0]	4.00[-1]	1.84[0]	2.87[0]	5.11[0]
40	3.35[-3]	3.35[-3]	8.15[-1]	1.05[0]	1.86[0]	2.50[-1]	1.39[0]	1.74[0]	3.38[0]
50	2.38[-3]	2.38[-3]	4.82[-1]	6.48[-1]	1.13[0]	1.59[-1]	1.02[0]	1.06[0]	2.24[0]
60	1.77[-3]	1.77[-3]	2.99[-1]	4.19[-1]	7.18[-1]	1.04[-1]	7.45[-1]	6.56[-1]	1.18[0]
80	1.06[-3]	1.06[-3]	1.28[-1]	1.94[-1]	3.22[-1]	5.16[-2]	4.04[-1]	2.70[-1]	7.25[-1]
100	6.77[-4]	6.77[-4]	6.05[-2]	9.88[-2]	1.59[-1]	2.97[-2]	2.27[-1]	1.22[-1]	3.79[-1]
200	1.33[-4]	1.33[-4]	3.49[-3]	7.68[-3]	1.12[-2]	4.91[-3]	2.10[-2]	6.17[-3]	3.21[-2]
	$4s$	$4p$	$4d$	$4f$	$Q(4)$	Total			
25	1.42[-1]	5.47[-1]	8.32[-1]	3.64[-1]	1.88[0]	1.26[+1]			
30	1.35[-1]	5.67[-1]	8.11[-1]	3.42[-1]	1.85[0]	1.03[+1]			
40	1.02[-1]	5.04[-1]	6.29[-1]	2.53[-1]	1.49[0]	6.76[0]			
50	7.13[-2]	4.04[-1]	4.40[-1]	1.71[-1]	1.08[0]	4.47[0]			
60	4.93[-2]	3.13[-1]	2.99[-1]	1.12[-1]	7.73[-1]	2.69[0]			
80	2.52[-2]	1.81[-1]	1.38[-1]	4.72[-2]	3.91[-1]	1.45[0]			
100	1.46[-2]	1.06[-1]	6.69[-2]	2.04[-2]	2.08[-1]	7.53[-1]			
200	2.36[-3]	1.02[-2]	3.73[-3]	6.56[-4]	1.69[-2]	6.03[-2]			

TABLE V. Total nl cross sections for $\text{Be}^{4+}\text{-H}(1s)$ ($a[b]$ stands for $a \times 10^b$).

Energy (keV/amu)	Cross sections (10^{-16} cm^2)								
	$1s$	$Q(1)$	$2s$	$2p$	$Q(2)$	$3s$	$3p$	$3d$	$Q(3)$
50	3.25[-2]	3.25[-2]	5.35[-1]	3.50[0]	4.03[0]	3.64[-1]	1.19[0]	3.91[0]	5.46[0]
60	2.48[-2]	2.48[-2]	3.31[-1]	2.44[0]	2.77[0]	2.37[-1]	8.69[-1]	2.42[0]	3.53[0]
80	1.58[-2]	1.58[-2]	1.48[-1]	1.30[0]	1.45[0]	1.07[-1]	5.07[-1]	1.02[0]	1.63[0]
100	1.09[-2]	1.09[-2]	7.82[-2]	7.57[-1]	8.35[-1]	5.27[-2]	3.17[-1]	4.75[-1]	8.45[-1]
200	2.48[-3]	2.48[-3]	1.22[-2]	9.42[-2]	1.06[-1]	5.57[-3]	4.64[-2]	2.71[-2]	7.91[-2]
500	1.96[-4]	1.96[-4]	8.54[-4]	2.11[-3]	2.96[-3]	3.41[-4]	1.02[-3]	2.41[-4]	1.60[-3]
	$4s$	$4p$	$4d$	$4f$	$Q(4)$	$5s$	$5p$	$5d$	$5f$
50	1.64[-1]	5.08[-1]	1.56[0]	1.63[0]	3.86[0]	8.09[-2]	4.15[-1]	7.14[-1]	8.50[-1]
60	1.16[-1]	3.85[-1]	1.09[0]	1.12[0]	2.71[0]	6.07[-2]	3.11[-1]	5.40[-1]	6.65[-1]
80	5.74[-2]	2.33[-1]	5.29[-1]	5.16[-1]	1.33[0]	3.21[-2]	1.85[-1]	2.88[-1]	3.56[-1]
100	2.92[-2]	1.49[-1]	2.65[-1]	2.38[-1]	6.81[-1]	1.68[-2]	9.28[-2]	1.51[-1]	1.79[-1]
200	2.82[-3]	2.33[-2]	1.65[-2]	8.89[-3]	5.15[-2]	1.56[-3]	9.65[-3]	9.91[-3]	7.43[-3]
500	1.61[-4]	5.06[-4]	1.51[-4]	2.55[-5]	8.43[-4]	8.65[-5]	2.08[-4]	9.05[-5]	2.14[-5]
	$5g$			$Q(5)$			Total		
50	2.78[-1]			2.33[0]			1.57[+1]		
60	2.20[-1]			1.80[0]			1.08[+1]		
80	1.13[-1]			9.97[-1]			5.43[0]		
100	5.28[-2]			4.92[-1]			2.86[0]		
200	1.45[-3]			2.99[-2]			2.70[-1]		
500	1.61[-6]			4.09[-4]			5.02[-3]		

where $a=Z-q$. All the terms in the transition matrix element may be generated by suitable parametric differentiation from a general term of the form as

$$\begin{aligned}
K = & \int d\vec{r}_T d\vec{R}_T e^{-i\vec{k}_f \cdot \vec{R}_T} \frac{e^{-\lambda r_P}}{r_P} {}_1F_1(i\nu_1; 1; ia(\nu_f r_T \\
& + \vec{\nu}_f \cdot \vec{r}_T)) {}_1F_1(-i\nu_2; 1; ib(k_f R_T + \vec{k}_f \cdot \vec{R}_T)) \\
& \times e^{i\vec{k}_i \cdot \vec{R}_T} \frac{e^{-\beta r_T}}{r_T}. \quad (10)
\end{aligned}$$

This six-dimensional integral may be reduced to a one-dimensional integral in compact form following an earlier investigation [18] by our group. Finally cross sections are obtained by integration over scattering angles. These integrals are performed numerically in a 24-point and a 48-point

Gauss Legendre quadrature method with an accuracy of 0.1%. However, it may be mentioned that sixth-order parametric differentiation of the final expression for ‘‘ K ’’ has been required to generate all the cross sections of our present investigation and has been performed analytically.

III. RESULTS AND DISCUSSIONS

Our calculated results for the partial and total charge-transfer cross section in the $\text{Be}^{q+}(q=1-4)+\text{H}$ interaction in different shells or subshells are given in Tables II–V and comparison with other available total charge transfer cross sections are displayed in Figs. 2–5, respectively. The same computed results for the $\text{B}^{q+}(q=1-5)+\text{H}$ interaction are shown in Tables VI–X and Figs. 6–10, respectively. Due to the nonavailability of experimental results in most of the cases comparisons are mainly confined to other theoretical

TABLE VI. Total nl cross sections for $\text{B}^+\text{-H}(1s)$ ($a[b]$ stands for $a \times 10^b$).

Energy (keV/amu)	Cross sections (10^{-16} cm^2)						
	$2p$	$Q(2)$	$3s$	$3p$	$3d$	$Q(3)$	Total
25	5.21[0]	5.21[0]	9.53[-2]	6.71[-2]	6.79[-3]	1.69[-1]	5.38[0]
30	4.04[0]	4.04[0]	9.20[-2]	5.99[-2]	6.00[-3]	1.58[-1]	4.19[0]
40	2.37[0]	2.37[0]	6.99[-2]	4.17[-2]	3.89[-3]	1.15[-1]	2.48[0]
50	1.45[0]	1.45[0]	4.66[-2]	2.66[-2]	2.29[-3]	7.55[-2]	1.52[0]
60	9.26[-1]	9.26[-1]	3.06[-2]	1.66[-2]	1.33[-3]	4.85[-2]	9.74[-1]
80	4.11[-1]	4.11[-1]	1.35[-2]	6.46[-3]	4.55[-4]	2.04[-2]	4.31[-1]
100	2.03[-1]	2.03[-1]	6.37[-3]	2.74[-3]	1.74[-4]	9.28[-3]	2.12[-1]
200	1.62[-2]	1.62[-2]	3.86[-4]	1.03[-4]	4.26[-6]	4.93[-4]	1.67[-2]

results only. In order to reduce the length of the tables, no numerical results obtained in BES and SS models are given in the tables. They are only compared in figures.

Charge-transfer cross sections into subshells of $n=2$ and $n=3$ in $\text{Be}^+ + \text{H}$ interaction are given in Table II. Due to the nonavailability of any other theoretical or experimental results for $\text{Be}^+ + \text{H}$ interaction, our computed results are compared in Fig. 2. From the table, we find that dominant cross sections come from the $n=2$ shell and the $n=3$ shell contributes around 5% to the total cross section. From Fig. 2 it is evident that all results have a converging trend towards higher energies and differ by a few factors at lower part of the energy range. Table III contains the subshell results of the $\text{Be}^{2+} + \text{H}$ interaction. Results for total cross sections are compared in Fig. 3 with CTMC results of Schultz *et al.* [10]. From Table III, we see that the maximum contribution comes from the $n=2$ shell and has a converging trend within 30% for capture into the $n=3$ shell. For each individual subshell, cross sections are favored into the p state, which is at parity with the observations of Schultz *et al.* [10]. However, we observe from Fig. 3 that at higher energies results of Schultz *et al.* [10] differ by a factor 2 and the discrepancy gradually diminishes towards lower energies. Our computed results in BES and SS screening methods have a similar pattern of energy variation. Charge transfer cross sections into each subshell are displayed in Table IV and total cross sections are compared in Fig. 4 for collision of Be^{3+} with atomic hydrogen. From the table, we see that maximum cross section is obtained from the $n=3$ shell and thereby have a converging trend within 25% for capture into $n=4$ shell. For this process our computed results are in good agreement with those of Schultz *et al.* [10] in regard to subshell distribution of the charge-transfer cross sections except for the fact that our cross sections attain their peak at the $3p$ state, in contrast to their maximum at the $2p$ state. As may be expected, our computed results in BES and SS models are almost identical and differ from the results obtained in the model potential approach. However, our computed total cross-section results are lower by a factor of 3 with those of Schultz *et al.* [10] at the highest energies and the discrepancy gradually diminishes significantly at lower energies. Results for collision of Be^{4+} with ground-state atomic hydrogen are given in Table V. From the table, we may find that maximum contribution comes from the $n=4$ shell. For each individual shell cross sections have attained their peak into the highest angular momentum state. This behavior is significantly dif-

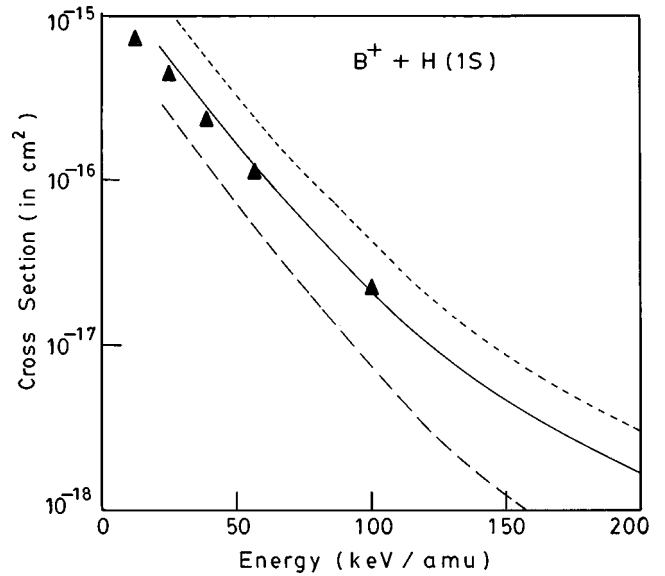


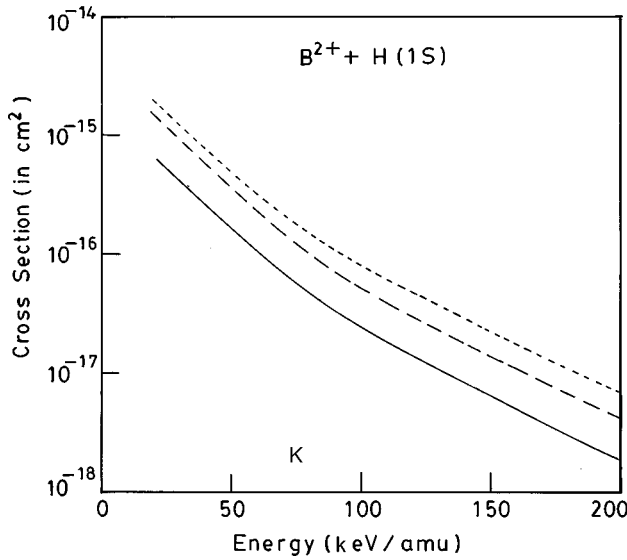
FIG. 6. Total capture cross sections for $\text{B}^+ + \text{H}(1s)$ collisions. Theory: —, present work (model potential); -----, present work (SS model); - - -, present work (BES model); ▲'s, the results of Hansen and Dubois [9].

ferent for other partially stripped ions of beryllium. Our computed results for total cross sections are in very good agreement with those of Schultz *et al.* [10] and fairly consistent with CDW-EFS results of Busnengo *et al.* [19].

Charge-transfer cross section into different subshells in collision of B^+ with ground-state atomic hydrogen are displayed in Table VI and total cross-section results are compared in Fig. 6. From the table, we find that the maximum contribution comes from the $n=2$ shell and is convergent within 5% for capture into the $n=3$ shell, which is in very good agreement with the computed results of Hansen and Dubois [9]. However, the subshell distributions of cross sections into the $n=3$ shell are in disagreement with each other though the net contribution from this shell is very small. Our other (BES and SS) results differ significantly. Table VII and Fig. 7 contain numerical and graphical results of the $\text{B}^{2+} + \text{H}$ interaction, respectively. Neither any theoretical nor any experimental results are available for this process. In this case the maximum cross section is obtained from the $n=2$ shell with a dominant contribution from the $2p$ state and the $n=3$ shell contributes around 35% to the total cross section. Our computed results in three different approaches have the

TABLE VII. Total nl cross sections for $\text{B}^{2+} - \text{H}(1s)$ ($a[b]$ stands for $a \times 10^b$).

Energy (keV/amu)	Cross sections (10^{-16} cm^2)							Total
	$2s$	$2p$	$Q(2)$	$3s$	$3p$	$3d$	$Q(3)$	
25	1.24[0]	2.24[0]	3.48[0]	2.25[-1]	9.01[-1]	4.20[-1]	1.55[0]	5.03[0]
30	9.09[-1]	1.63[0]	2.54[0]	2.02[-1]	8.62[-1]	3.93[-1]	1.46[0]	4.00[0]
40	5.20[-1]	9.28[-1]	1.45[0]	1.49[-1]	6.59[-1]	2.76[-1]	1.08[0]	2.53[0]
50	3.18[-1]	5.62[-1]	8.80[-1]	1.08[-1]	4.57[-1]	1.73[-1]	7.38[-1]	1.62[0]
60	2.04[-1]	3.59[-1]	5.63[-1]	7.84[-2]	3.09[-1]	1.06[-1]	4.93[-1]	1.06[0]
80	9.31[-2]	1.64[-1]	2.57[-1]	4.27[-2]	1.42[-1]	4.11[-2]	2.26[-1]	4.83[-1]
100	4.70[-2]	8.34[-2]	1.30[-1]	2.44[-2]	6.83[-2]	1.71[-2]	1.10[-1]	2.40[-1]
200	3.59[-3]	7.16[-3]	1.07[-2]	2.62[-3]	3.85[-3]	6.03[-4]	7.07[-3]	1.78[-2]

FIG. 7. Same as in Fig. 2 for $B^{2+}+H(1s)$ collisions.

same energy variation except in magnitude. Numerical results for collision of B^{3+} with atomic hydrogen are displayed in Table VIII and graphical comparisons are drawn in Fig. 8. From the table we observe that charge transfer into the $n=3$ shell is most favored and thereby decreases by a 25% contribution from the $n=4$ shell to the total cross sections. At lower energies the $3d$ state dominates and with increasing impact energy the $3p$ state overcomes the situation. From Fig. 8 we see that our computed results for total capture cross sections in the model potential approach have excellent agreement with those of Hansen and Dubois [9]. CTMC results of Olson and Salop [8] have discrepancies with our observation in the model potential approach but have fair

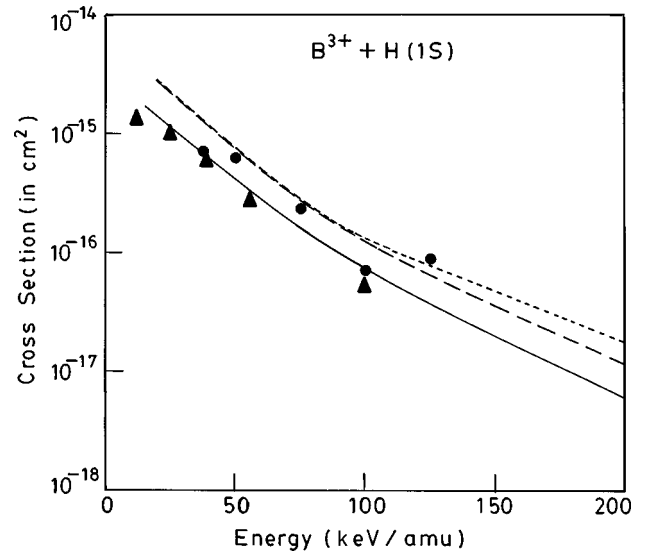


FIG. 8. Total capture cross sections for $B^{3+}+H(1s)$ collisions. Theory: —, present work (model potential); , present work (SS model); (— —), present work (BES model); ▲'s, the results of Hansen and Dubois [9]; and ●'s, CTMC results of Olson and Salop *et al.* [8].

agreement with our results in BES and SS models. From Table IX, we find that charge-transfer cross sections for collision of B^{4+} with atomic hydrogen have a maximum value at the $n=4$ shell at low energies and as impact energy increases the contribution from the $n=3$ shell becomes dominating over all other shells. Capture into the $3d$ subshell is mostly favorable for the $n=3$ shell except at highest energy. On the other hand, the $4f$ subshell contribution is maximum at low energies and this maximum gradually shifted towards

TABLE VIII. Total nl cross sections for $B^{3+}-H(1s)$ ($a[b]$ stands for $a \times 10^b$).

Energy (keV/amu)	Cross section (10^{-16} cm^2)						
	$2s$	$2p$	$Q(2)$	$3s$	$3p$	$3d$	$Q(3)$
25	9.69[−1]	1.57[0]	2.54[0]	5.09[−1]	2.05[0]	3.42[0]	5.98[0]
30	7.12[−1]	1.15[0]	1.86[0]	4.02[−1]	1.85[0]	2.60[0]	4.85[0]
40	4.15[−1]	6.65[−1]	1.08[0]	2.46[−1]	1.40[0]	1.76[0]	3.41[0]
50	2.59[−1]	4.14[−1]	6.73[−1]	1.55[−1]	1.03[0]	1.09[0]	2.27[0]
60	1.70[−1]	2.70[−1]	4.40[−1]	1.01[−1]	7.57[−1]	6.78[−1]	1.54[0]
80	8.10[−2]	1.27[−1]	2.08[−1]	4.98[−2]	4.12[−1]	2.82[−1]	7.44[−1]
100	4.23[−2]	6.64[−2]	1.09[−1]	2.85[−2]	2.31[−1]	1.28[−1]	3.87[−1]
200	3.54[−3]	5.73[−3]	9.27[−3]	4.70[−3]	2.13[−2]	6.42[−3]	3.24[−2]
	$4s$	$4p$	$4d$	$4f$	$Q(4)$	Total	
25	1.41[−1]	5.22[−1]	7.58[−1]	3.00[−1]	1.72[0]	1.02[+1]	
30	1.34[−1]	5.54[−1]	7.67[−1]	2.96[−1]	1.75[0]	8.46[0]	
40	1.02[−1]	5.06[−1]	6.22[−1]	2.31[−1]	1.46[0]	5.95[0]	
50	7.15[−2]	4.12[−1]	4.47[−1]	1.60[−1]	1.09[0]	4.03[0]	
60	4.95[−2]	3.22[−1]	3.08[−1]	1.07[−1]	7.86[−1]	2.77[0]	
80	2.54[−2]	1.88[−1]	1.44[−1]	4.58[−2]	4.03[−1]	1.35[0]	
100	1.47[−2]	1.10[−1]	7.00[−2]	2.00[−2]	2.15[−1]	7.11[−1]	
200	2.38[−3]	1.06[−2]	3.89[−3]	6.61[−4]	1.75[−2]	5.92[−2]	

TABLE IX. Total nl cross sections for $B^{4+}-H(1s)$ ($a[b]$ stands for $a \times 10^b$).

Energy (keV/amu)	Cross sections (10^{-16} cm 2)								
	$1s$	$Q(1)$	$2s$	$2p$	$Q(2)$	$3s$	$3p$	$3d$	$Q(3)$
25	1.37[-3]	1.37[-3]	2.94[-1]	3.01[-1]	5.95[-1]	1.13[0]	3.59[0]	1.52[1]	1.99[1]
30	1.11[-3]	1.11[-3]	2.19[-1]	2.24[-1]	4.43[-1]	8.56[-1]	2.72[0]	1.14[1]	1.50[1]
40	7.90[-4]	7.90[-4]	1.32[-1]	1.36[-1]	2.68[-1]	5.14[-1]	1.69[0]	6.56[0]	8.76[0]
50	5.97[-4]	5.97[-4]	8.65[-2]	8.92[-2]	1.76[-1]	3.22[-1]	1.15[0]	3.92[0]	5.39[0]
60	4.68[-4]	4.68[-4]	5.93[-2]	6.16[-2]	1.21[-1]	2.08[-1]	8.32[-1]	2.43[0]	3.47[0]
80	3.09[-4]	3.09[-4]	3.06[-2]	3.25[-2]	6.31[-2]	9.44[-2]	4.81[-1]	1.02[0]	1.59[0]
100	2.18[-4]	2.18[-4]	1.72[-2]	1.88[-2]	3.60[-2]	4.72[-2]	3.00[-1]	4.74[-1]	8.21[-1]
200	5.63[-5]	5.63[-5]	1.89[-3]	2.39[-3]	4.28[-3]	5.14[-3]	4.41[-2]	2.69[-2]	7.61[-2]
	$4s$	$4p$	$4d$	$4f$	$Q(4)$	$5s$	$5p$		
25	3.24[-1]	9.45[-1]	3.07[0]	3.22[0]	7.56[0]	1.04[-1]	9.67[-1]		
30	2.97[-1]	8.76[-1]	2.89[0]	3.02[0]	7.08[0]	1.11[-1]	1.06[0]		
40	2.24[-1]	6.75[-1]	2.22[0]	2.34[0]	5.45[0]	1.01[-1]	9.74[-1]		
50	1.59[-1]	5.03[-1]	1.58[0]	1.66[0]	3.90[0]	8.02[-2]	7.08[-1]		
60	1.12[-1]	3.79[-1]	1.10[0]	1.14[0]	2.73[0]	5.97[-2]	5.18[-1]		
80	5.46[-2]	2.28[-1]	5.31[-1]	5.22[-1]	1.34[0]	3.13[-2]	2.03[-1]		
100	2.78[-2]	1.45[-1]	2.65[-1]	2.40[-1]	6.79[0]	1.64[-2]	1.05[-1]		
200	2.71[-3]	2.26[-2]	1.65[-2]	8.93[-3]	5.07[-2]	1.53[-3]	2.06[-2]		
	$5d$	$5f$	$5g$	$Q(5)$	Total				
25	8.66[-1]	8.97[-1]	2.61[-1]	3.09[0]	3.11[1]				
30	9.60[-1]	1.02[0]	2.99[-1]	3.45[0]	2.59[1]				
40	9.00[-1]	1.03[0]	3.24[-1]	3.33[0]	1.78[1]				
50	7.23[-1]	8.74[-1]	2.89[-1]	2.67[0]	1.21[1]				
60	5.45[-1]	6.81[-1]	2.27[-1]	2.03[0]	8.35[0]				
80	2.89[-1]	3.62[-1]	1.16[-1]	1.10[0]	4.09[0]				
100	1.52[-1]	1.81[-1]	5.37[-2]	5.08[-1]	2.04[0]				
200	9.87[-3]	7.48[-3]	1.46[-3]	4.09[-2]	1.72[-1]				

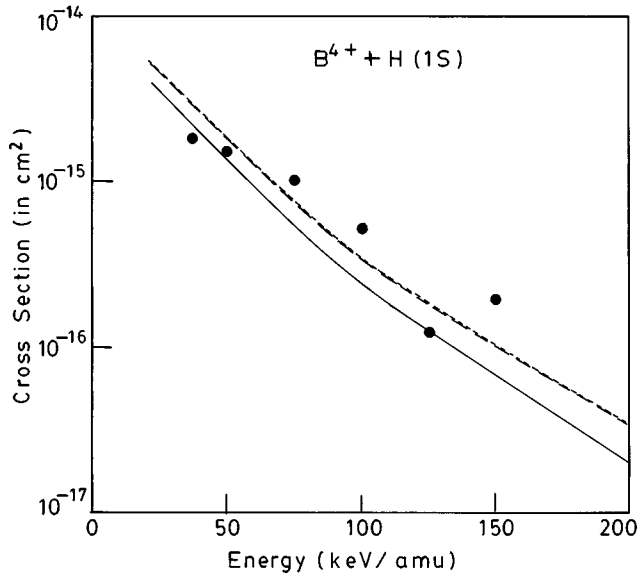


FIG. 9. Total capture cross sections for $B^{4+}+H(1s)$ collisions. Theory: —, present work (model potential); , present work (SS model); (- - -), present work (BES model); and ●●●●●, CTMC results of Olson and Salop *et al.* [8].

the $4d$ state as projectile energy increases. Contribution from the $n=5$ shell is around 20%. For the same process, we find from Fig. 9 that CTMC results of Olson and Salop [8] have close agreement only at lower energies but consistencies disappear at high energies in comparison to our results. However, the disagreement among our computed results reduces as the charge on the projectile ion increases. Our computed results for charge transfer cross sections in the $B^{5+}+H$ interaction are displayed in Table X and graphical comparisons are drawn in Fig. 10. From the table, it is evident that maximum capture takes place into the $n=4$ shell and has a converging trend towards higher shells having a contribution around 30% from the $n=5$ shell. From Fig. 10, we see that our computed results are in excellent agreement with the experimental observations of Goffe *et al.* [5]. Computed results in the CDW-EFS approximation of Busnengo *et al.* [19] are lower by a factor of 2 over the entire region. However, results of Hansen and Dubois [9] in the coupled state calculation are lower by a factor of 5 at low energies and the discrepancy enhances with increasing projectile energy.

Though we have not shown in the tables, the cross sections are found to be maximum at the $m=0$ state for a given value of l and n in all the cases. This corresponds to the

TABLE X. Total nl cross sections for $B^{5+}-H(1s)$ ($a[b]$ stands for $a \times 10^b$).

Energy (keV/amu)	Cross sections (10^{-16} cm 2)					
	$1s$	$Q(1)$	$2s$	$2p$	$Q(2)$	$3s$
50	1.69[-2]	1.69[-2]	6.01[-1]	2.86[0]	3.46[0]	5.44[-1]
60	1.34[-2]	1.34[-2]	3.82[-1]	2.07[0]	2.45[0]	3.70[-1]
80	9.10[-3]	9.10[-3]	1.77[-1]	1.18[0]	1.36[0]	1.85[-1]
100	6.56[-3]	6.56[-3]	9.32[-2]	7.39[-1]	8.32[0]	9.81[-2]
200	2.08[-3]	2.08[-3]	1.16[-2]	1.22[-1]	1.34[-1]	8.14[-3]
500	2.07[-4]	2.07[-4]	9.63[-4]	4.27[-3]	5.23[-3]	4.06[-4]
	$3p$	$3d$	$Q(3)$	$4s$	$4p$	$4d$
50	1.52[0]	1.30[1]	1.51[1]	2.66[-1]	7.76[-1]	6.22[0]
60	9.99[-1]	8.19[0]	9.56[0]	1.94[-1]	5.39[-1]	4.42[0]
80	5.19[-1]	3.56[0]	4.26[0]	1.07[-1]	2.82[-1]	2.23[0]
100	3.17[-1]	1.69[0]	2.10[0]	5.99[-2]	1.66[-1]	1.15[0]
200	6.06[-2]	9.97[-2]	1.68[-1]	4.96[-3]	3.07[-2]	7.15[-2]
500	2.27[-3]	8.98[-4]	3.57[-3]	1.96[-4]	1.16[-3]	5.80[-4]
	$4f$	$Q(4)$	$5s$	$5p$	$5d$	$5f$
50	1.10[1]	1.85[1]	1.29[-1]	7.06[-1]	2.70[0]	5.77[0]
60	7.64[0]	1.28[1]	1.01[-1]	5.15[-1]	2.16[0]	4.58[0]
80	3.62[0]	6.24[0]	5.97[-2]	2.16[-1]	1.25[0]	2.58[0]
100	1.75[0]	3.12[0]	3.51[-2]	1.04[-1]	6.94[-1]	1.37[0]
200	7.82[-2]	1.85[-1]	3.05[-3]	2.37[-2]	4.63[-2]	7.02[-2]
500	2.38[-4]	2.17[-3]	1.06[-4]	8.69[-4]	3.54[-4]	2.09[-4]
	$5g$	$Q(5)$	Total			
50		3.07[0]	1.24[1]	4.95[1]		
60		2.37[0]	9.70[0]	3.45[1]		
80		1.24[0]	5.34[0]	1.72[1]		
100		6.05[-1]	2.81[0]	8.86[0]		
200		2.08[-2]	1.64[-1]	6.51[-1]		
500		2.75[-5]	1.54[-3]	1.27[-2]		

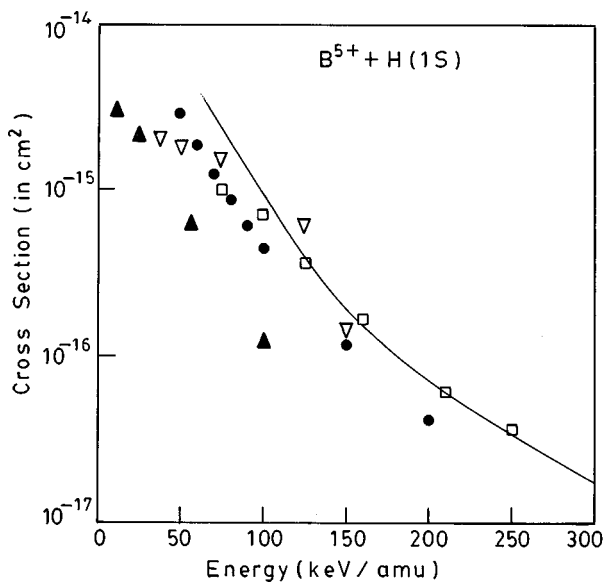


FIG. 10. Total capture cross sections for $B^{5+}+H(1s)$ collisions. Theory: —, present theory; $\nabla\nabla\nabla\nabla$, CTMC results of Olson and Salop [8]; $\blacktriangle\blacktriangle\blacktriangle$, the results of Hansen and Dubois [9]; $\bullet\bullet\bullet\bullet$, the results of CDW-EFS of Busnengo *et al.* [19]. Expt.: $\square\square\square\square$, the results of Goffe *et al.* [5].

classical picture that the electron is mostly captured into orbitals in collisional plane and this behavior is also in conformity with the previous calculation [20]. It is evident from the tables that cross sections have peak values at particular values of l and n . This may be justified by the energy resonance of the electron in the initial and final state. However, this justification is little altered when the asymptotic charge on the projectile ion exceeds three, which may be explained in terms of Landau-Zener dynamics.

IV. CONCLUDING REMARKS

State selective capture cross sections have been calculated in the framework of boundary corrected continuum intermediate state (BCCIS) approximation in collisions of all possible ions of beryllium and boron with ground-state atomic hydrogen. For closed-shell structure of the projectile ion, our results obtained in three different models are consistent with a certain degree of accuracy but disagreement is pronounced for projectile ions having open shell structure. This feature indicates that in the case of studies on charge-transfer processes involving partially stripped ions of open-shell structure with atoms, much care has to be taken in describing the interaction of the active electron with the projectile ion. Fair

agreement of our computed results in the model potential approach in the BCCIS approximation with other existing theoretical and experimental results (limited to fully stripped boron ion only) indicate the reliability and accuracy of our method in intermediate- and high-energy region. However, experimental results for such processes are highly needed under the prevailing circumstances.

ACKNOWLEDGMENTS

One of us (C.R.M.) would like to thank the Department of Science and Technology (Government of India), New Delhi, India for their support of this work through Grant No. SP/S2/L03/95. The authors are grateful to Professor S. C. Mukherjee for his valuable comments.

-
- [1] J. S. Briggs and J. H. Macek, *Adv. At., Mol., Opt. Phys.* **28**, 1 (1990).
- [2] W. Fritsch and C. D. Lin, *Phys. Rep.* **202**, 1 (1991).
- [3] D. S. F. Crothers and L. J. Dube, *Adv. At., Mol., Opt. Phys.* **30**, 287 (1992).
- [4] D. Belkic, R. Gayet, and A. Salin, *At. Data Nucl. Data Tables* **51**, 59 (1992).
- [5] T. V. Goffe, M. B. Shah, and H. B. Gilbody, *J. Phys. B* **12**, 3763 (1979).
- [6] H. K. Haugen, L. H. Andersen, P. Hvelplund, and H. Knudsen, *Phys. Rev. A* **26**, 1950 (1982).
- [7] *Atomic and Molecular Processes in Fusion Edge Plasmas*, edited by R. K. Janev (Plenum, Press, New York, 1995).
- [8] R. E. Olson and A. Salop, *Phys. Rev. A* **16**, 531 (1977).
- [9] J. P. Hansen and A. Dubois, *Phys. Scr.* **T62**, 55 (1996).
- [10] D. R. Schultz, P. S. Krstic, and C. O. Reinhold, *Phys. Scr.* **T62**, 69 (1996).
- [11] C. R. Mandal, Mita Mandal, and S. C. Mukherjee, *Phys. Rev. A* **44**, 2968 (1991).
- [12] S. Datta, D. S. F. Crothers, and R. McCarroll, *J. Phys. B* **23**, 479 (1990).
- [13] F. Decker and J. Eichler, *Phys. Rev. A* **39**, 1530 (1989).
- [14] C. R. Mandal, Mita Mandal, and S. C. Mukherjee, *Phys. Rev. A* **42**, 1803 (1990).
- [15] C. A. Coulson, *VALANCE* (Oxford University Press, Oxford, 1963), p. 40.
- [16] E. Clementi and C. Roetti, *At. Data Nucl. Data Tables* **14**, 185 (1974).
- [17] R. E. H. Clark and J. Abdallah, Jr., *Phys. Scr.* **T62**, 7 (1996).
- [18] M. Ghosh, C. R. Mandal, and S. C. Mukherjee, *Phys. Rev. A* **35**, 2815 (1987).
- [19] H. F. Busnengo, S. E. Corchs, A. E. Martinez, and R. D. Rivarola, *Phys. Scr.* **T62**, 88 (1996).
- [20] H. Ryufuku and T. Watanabe, *Phys. Rev. A* **20**, 1828 (1979).